Arabian Journal of Chemistry (2021) **14**, 103111

King Saud University

Arabian Journal of Chemistry

www.ksu.edu.sa
www.sciencedirect.com

ORIGINAL ARTICLE

Preparation and characterization of guar gum based biopolymeric hydrogels for controlled release of antihypertensive drug

Hina Daud [a,b], Ambreen Ghani [c], Dure Najaf Iqbal [d], Nasir Ahmad [e], Saliha Nazir [a,b], Mahnoor Jan Muhammad [a], Erum Akbar Hussain [a,f,*], Arif Nazir [d], Munawar Iqbal [d,*]

[a] *Department of Chemistry, Lahore College for Women University, Lahore 54000, Pakistan*
[b] *Roy & Diana Vagelos Laboratories, Department of Chemistry, University of Pennsylvania, Philadelphia, PA 19104, United States*
[c] *Department of Chemistry, University of Education Lahore, Vehari Campus 61100, Pakistan*
[d] *Department of Chemistry, University of Lahore, Lahore 53700, Pakistan*
[e] *Department of Biomedical Engineering and Sciences, School of Mechanical and Manufacturing Engineering, National University of Science & Technology, Islamabad, Pakistan*
[f] *H.E.J Research Institute of Chemistry, University of Karachi, Karachi, Pakistan*

Received 3 January 2021; accepted 2 March 2021
Available online 12 March 2021

KEYWORDS

Guar gum;
Hydrogels;
Solution casting technique;
Anti-hypertensive drug;
Controlled drug release

Abstract Rapid release and poor drug encapsulation ability limit the use of single biopolymer in water-soluble drugs loading, carrying and release efficiency. In the present study, blended hydrogels based on guar gum, sodium alginate and polyvinyl alcohol (GG/SA/PVA) were prepared by solution casting technique and employed for controlled release of verapamil HCl (VP-HCl). The extent of interaction of all blends was explored by Fourier-transform infrared spectroscopy (FTIR) while surface morphology was determined by Atomic force microscope (AFM) and Scanning electron microscope (SEM). The crystallinity, thermal stability and water absorbing capacity of blends were studied by X-ray diffraction (XRD), Differential scanning calorimeter (DSC), thermogravimetric analysis (TGA) and swelling studies respectively. The results revealed improved crystallinity and stability of all the blends. The prepared blends showed promising drug loading and releasing efficiency with higher GG contents for the controlled release of verapamil HCl and at pH 7.4. Optimum drug release (94%) drug release was achieved in 12 h and followed non-Fickian diffusion

* Corresponding authors.
E-mail addresses: erum.hussain@gmail.com (E.A. Hussain), munawar.iqbal@chem.uol.edu.pk (M. Iqbal).
Peer review under responsibility of King Saud University.

Production and hosting by Elsevier

https://doi.org/10.1016/j.arabjc.2021.103111

mechanism. It has been concluded from the results that GG/SA/PVA blends have potential for drug delivery applications in a controlled manner.

1. Introduction

Hypertension is often accompanied with cardiac disorders and considered as third most life threatening disease (Prasanth et al., 2020). Verapamil hydrochloride is an antihypertensive drug that prevents the entry of calcium in cardiac cells resulting in lowering of blood pressure. The approximate low bioavailability is due to rapid biotransformation in the liver having biological half-life of 4.2 h, thus require increased dosage of drug. Therefore, sustained release of verapamil is required for improved compliance in patient in order to ensure effective therapy. Hydrogels being polymeric networks, have ability to absorb biological fluids and water (Hu et al., 2020a, b; Hu et al., 2017). Therefore, hydrogels have become excellent drug carriers especially for water soluble drugs (Abdullah et al., 2018; Ahmad et al., 2020; Akbari et al., 2020; Nesrinne and Djamel, 2017). Literature review revealed many hydrogels employed in their pristine and modified forms including starch, cellulose, guar gum, chitosan and sodium alginate in biomedical applications (Abbas et al., 2019; Iqbal et al., 2020c). Natural polymers are often preferred owing to low cost, free availability, non-toxic nature and biodegradability over the synthetic polymers. Though, they have few drawbacks that can be controlled by applying some modifications like uncontrolled hydration, viscosity drop and microbial contamination on storing. Blending of biopolymers is one of the smart approach to improve the required characteristics of natural polymers and make them attractive biomaterial for controlled drug release (Abbas et al., 2019; Boukhouya et al., 2018; Iqbal and Khera, 2015; Samarth et al., 2015).

A non-ionic polysaccharide, guar gum (GG), is a promising molecule due to its diverse applications (Iqbal et al., 2020a; Iqbal et al., 2020b; Iqbal et al., 2020c). The (1–4)-linked-d-mannopyranose units were configured at 1 and 6 positions to d-galactose at branch points in GG. It serves as a binder and disintegrating agent in solid while it provides stabilization and thickness in liquid pharmaceutical formulations (Aminabhavi et al., 2014; Sharma et al., 2018). Sodium alginate (SA) is a hydrophilic, non-toxic and biodegradable polysaccharide isolated from brown sea weed in which 1–4 linked α-L-guluronic are alternate to β-D-mannuronic acid residues (Rasool et al., 2020; Thakur et al., 2018). A non-toxic, synthetic polymer polyvinyl alcohol (PVA), has been used in biomedical applications such as in artificial intestines, kidneys and blood vessels (Ailincai et al., 2020).

However, ultrapure biopolymer hydrogels show some drawbacks such as, poor mechanical strength, erodibility at alkaline pH and high hydrophilicity. These shortcomings can be overcome either by cross-linking or interpenetrating networks (IPNs) formation (Dhand et al., 2020; Park et al., 2017). In the large array of drug delivery systems (DDS), blended hydrogels have been emerged as one of the most implied matrices for the controlled release of drugs (Alpaslan et al., 2021; Campos et al., 2021; Mauri et al., 2021; Paradee et al., 2021). In the swollen condition, they resemble living tissue in softness and flexibility thus possess excellent biocompatibility (Ata et al., 2020; Iqbal et al., 2020b; Iqbal et al., 2020c; Nagpal et al., 2013a; Soppirnath and Aminabhavi, 2002). Some work on guar gum and sodium alginate with PVA combination as DDS have been studied for controlled release of different drugs (Grekhnyova et al., 2017; Pallavi and Pallavi, 2017; Rangaraj et al., 2010). To the best of our knowledge, the use of GG/SA/PVA blended hydrogels is the most recent one in the field.

Based on aforementioned facts, present study was designed to prepare a series of blended hydrogels based on, guar gum, sodium alginate and polyvinyl alcohol by solution casting method. The hydrogel blends were studied for drug loading and release efficiencies as a function of pH. The characterization of hydrogels was performed by FTIR, XRD, AFM, SEM, TGA/DSC and swelling properties.

2. Materials and methods

Pharmaceutical grade guar gum (GG), sodium alginate (SA) and polyvinyl alcohol (PVA) were purchased from Sigma Aldrich, Germany. Verapamil Hydrochloride (VP-HCl) was obtained from Searle, Pakistan. All analytical grade chemicals were used in the experiments and solutions preparation was accomplished in deionized water.

2.1. Preparation of hydrogels

The blended hydrogels were prepared by varying the concentration of GG and SA (0: 0.8, 0.2: 0.6, 0.4: 0.4, 0.6: 0.2, 0.8: 0, 0.5: 0.5 w/w) with fixed amount of PVA (0.2 g) by solution-casting technique at 50–60 °C. Both polymers were separately dissolved in deionized water (50 mL). PVA was dissolved in water (20 mL) with continuous stirring at 90 °C until no crystal left behind. After attaining complete solubility, all the solutions were mixed and allowed to react for 3 h. Then, blended hydrogel was poured in petri dish and dried at 40 °C.

2.2. Characterization

Spectro-analytical techniques were used for the confirmation of chemical structures of all the products. Fourier transform infrared (FTIR) spectra were recorded on Fourier Transformation Infrared spectrophotometer (scanning range 650–4000) Agilent Technologies. XRD patterns were measured on D8 Discover diffractometer, Bruker, Germany. Atomic force microscope (Agilent Technologies, 5500, mode; ACAFM, probe; mica sheets, resonance frequency; 298.563 kHz) was used to obtain the micrographs of the sample up to 0.5 μm. SEM micrographs were obtained using the ZEISS scanning electron microscope with the HDBSD detector. Atomic force microscope (Agilent Technologies, 5500,

Mode; ACAFM, Probe; Mica sheets, Resonance frequency; 298.563 kHz). UV–Visible spectrophotometer (UV–Vis-730: scanning speed; 10–400 nm/min, wavelength range; 190 to 1100 nm, light source; halogen lamp, deuterium lamp) was employed to record absorbance. The thermal behavior was studied by DSC/TGA, SDT-Q600TA Instrument, USA, from 25 °C to 600 °C at 10 °C /min heating rate (End down).

2.3. Swelling measurements

Completely dried blended hydrogels were weighed and kept in excess of swelling medium; distilled water, pH 1.2 and 7.4, respectively at 37 °C, then the swelled hydrogel was weighed after every 15 min. The swelling percent was calculated as shown in Eq. (1). Where, Ws and W_d are the masses of swollen and dried hydrogels, respectively. The experiments were accomplished in triplicates for each sample and standard deviation was exercised to express error. (George and Abraham, 2007).

$$Swelling\,\% = \frac{W_s - W_d}{W_d} \times 100 \quad (1)$$

2.4. Drug loading and release studies

Drug loading and release activity was performed on blended hydrogel samples. In this method, antihypertensive drug, VP-HCl was loaded in the mass ratio of 3:1 on the prepared hydrogel. A required quantity of VP-HCl was dissolved in small amount of deionized water and loaded on the hydrogel with constant stirring around 40–50 °C for 24 h. The drug loaded samples (GAV-02, GAV-03, GAV-04 and GAV-05) were washed with deionized water and dried in hot air oven for 3 h at 40 °C.

The VP-HCl content in the prepared hydrogel blends was assessed spectrophotometrically. The drug loaded sample (5 mg) was immersed in phosphate buffer (50 mL, pH 7.4) and shaken at room temperature for 24 h on a shaker (100 rpm). Then, the solution was centrifuged for 15 min at 2000 rpm, filtered and rinsed with fresh phosphate buffer. In a quartz cuvette, the amount of VP-HCl in filtrate was quantified by UV–Vis Spectrometer at λmax 278 nm. The experiments were accomplished in triplicates for each sample and standard deviation was exercised to express error. Drug loading (DL) and drug loading efficiency (DLE) were calculated

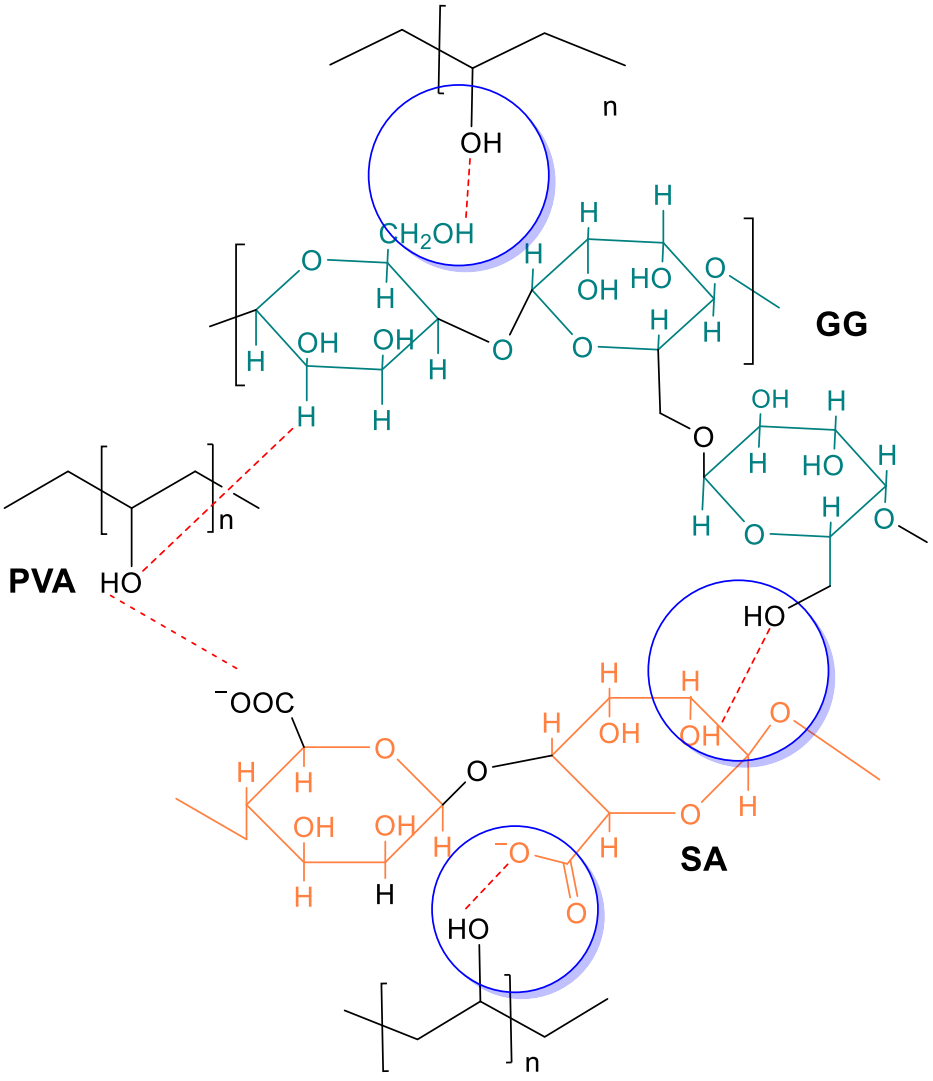

Fig. 1 Proposed interactions among polymers for the formation of blended hydrogels.

according to Eq. (2). Where, M_D is the mass of the drug (mg) in the hydrogel and M_{HG} is the mass of the hydrogel (mg). DLE was measured as depicted in Eq. (3) (Parandhama et al., 2017). Where, HG_{AL} is the actual loading of the drug on hydrogel and HG_{TL} is the theoretical loading.

$$DL\% = \frac{M_D}{M_{HG}} \times 100 \quad (2)$$

$$DLE\% = \frac{HG_{AL}}{HG_{TL}} \times 100 \quad (3)$$

The drug release responses of hydrogels were performed in phosphate buffer solution (PBS) at pH 1.2 and 7.4 while the physiological temperature was kept at 37 ± 0.5 °C. Prior to release experiments, the dialysis tubes (4 cm each) were plunged in distilled water for 2 h to remove preservatives. All tubes were dipped in the PBS after exhaustive rinsing with water to equilibrate for an hour. Afterward, the dialysis tube was filled with release medium (5 mL) followed by 5 mg of loaded sample of VP-HCl, sealed, shaken and instantly soaked in the release medium (25 mL), at 37 °C. This release medium (3 mL) aliquot was drawn at regular time intervals till 24 h and replaced with the fresh buffer solution. The experiments carried out at pH 1.2 were recorded with 15 min interval for 2.5 h while pH 7.4 was first observed at 30 min and then with 2 h interval respectively for 24 h. The buffer solution having VP-HCl content was measured using UV–Vis spectrophotometer at 278 nm. Three recurring observations were recoded for each sample and concurrent reading was used in calculations. All the drug release experiments were performed three times. Amount of VP-HCl released was calculated as depicted in Eq. (4). Where, D_R is the amount of VP-HCL released at a time interval (mg) and D_L is the total amount of VP-HCl loaded on the hydrogel (Sekhar et al., 2011).

$$VP - HCl\% = \frac{D_R}{D_L} \times 100 \quad (4)$$

2.5. Drug release kinetics

Different mathematical models were used to understand the rate and mechanism of drug release from the blended hydrogels. These are as follows:

Zero-order kinetics:

$$C_t/C_0 = K_0 t$$

Where C_t is the released amount of drug at time t and C_0 is the amount of drug released at t = 0 and K_0 is the rate constant for zero-order.

1st order kinetics:

$$\ln(1 - C_t/C_0) = -K_1 t$$

where C_t/C_0 is the fraction of drug release in time t and K_1 is the rate constant for 1st order.

Higuchi equation:

$$C_t/C_0 = K_h t^{1/2}$$

where C_t/C_0 is the fraction of drug release in time t and K_h is the rate constant for Higuchi equation.

Krosmeyer-Peppas equation:

$$M_t/M_\alpha = K_{kp} t^n$$

Where M_t/M_α is the fraction of drug release at time t, n is the release exponent and K_{kp} is the Krosmeyer-Peppas rate constant at time t^n which represents the geometric and structural characteristics of the hydrogels. For n = 0.5, the rate of drug release is Fickian and 0.5 < n less than 1, the drug release rate

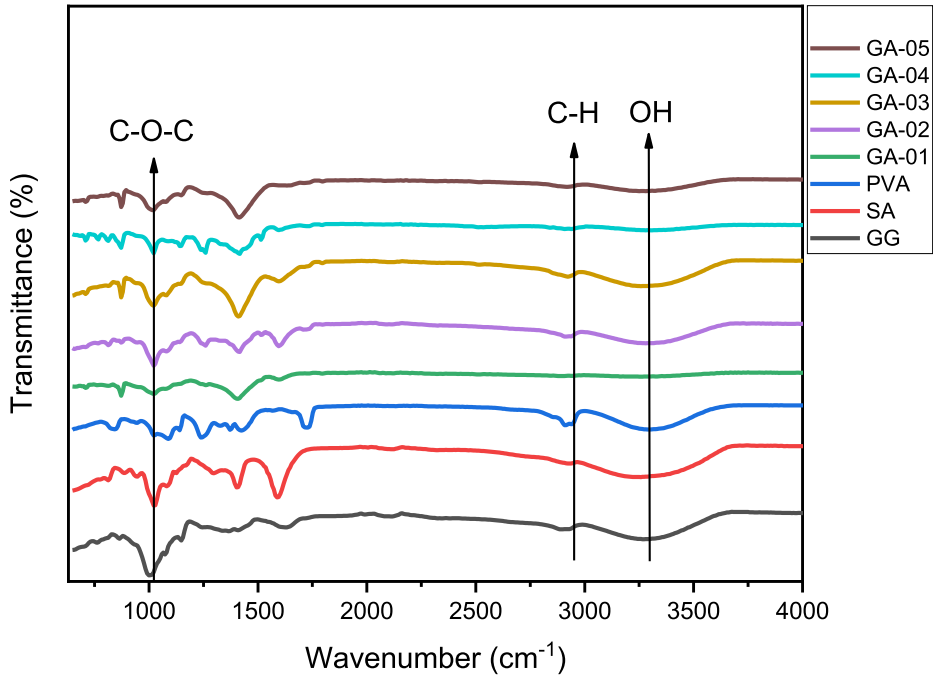

Fig. 2 FTIR Spectra of pristine polymers and blended hydrogels showing functional groups.

shows the anomalous Non-Fickian transport. If n = 1, the mechanism is case II transport (Paarakh et al., 2018).

3. Results and discussion

The optically clear homogeneous blends of GG/NaAlg/PVA were obtained by solution casting method. All blends revealed significant effect of polymer concentration with respect to crystallinity and water holding capacity supported by results of surface topology. The proposed mechanism (Fig. 1) involves the inter molecular H-bonding between GG and SA where PVA served as a physical crosslinker. It encompasses strong H-bonding between –OH of GG and $–COO^-$ ion of SA, –OH of PVA and $–COO^-$ of SA, –H of GG and $–COO^-$ of SA. The FTIR results completely supported blend formation by showing hydrogen bonding as cohesive forces.

3.1. FTIR studies of blended hydrogels

The FTIR analysis was performed to identify the functional groups (Amer and Awwad, 2021; Awwad and Amer, 2020) and on the basis of frequency shift in FTIR (Fig. 2), the formation of blends based on GG, SA and PVA polymers was fully supported. PVA was kept fixed in order to investigate the effect of varying concentrations of GG. In FTIR spectra, all the samples (GA-01 to GA-05) showed the broad band at 3257–3309 cm^{-1} which fairly match with pristine polymers 3257–3295 cm^{-1}. The stretching vibration at 2892–2937 cm^{-1} corresponded to sp^3 C-H stretch and the band at 872–879 cm^{-1} due to mannose units, 1–4 linkage remained unchanged indicating stability of biopolymer during blend formation. The strong absorption bands observed at 1000–1021 cm^{-1} attributed to C–O stretch of glycosidic linkage. Two prominent bands at 1595 and 1408–1416 cm^{-1} were attributed to asymmetric and symmetric carboxyl stretch respectively (Table 1) (Kajjari et al., 2012; Seeli et al., 2016). VP-HCl showed significant bands at 1453, 2944 and 1140 cm^{-1} corresponding to NH, $–CH_3$ and C–O–C stretch respectively. While bands at 1587 and 1513 cm^{-1} were attributed to the stretching of C=C group (Suardi et al., 2016). In drug loaded hydrogel blends all the peaks have been appeared with the slight shifting which shows that the VP-HCl is loaded successfully in the blends (Fig. 3).

3.2. Crystallinity study

The crystallinity was evaluated by XRD analysis (Shammout and Awwad, 2021) of pure polymers and blended hydrogels (GA-03, GA-04 and GA-05) and outcome were shown in Fig. 4. It is evident from the XRD results that GG showed mostly the amorphous region. The SA showed a strong peak at 2θ = 7.79° while PVA showed peaks at 7.97° and 19.58°. The minor shift in 2θ manifested the hydrogen bonding interactions between the GG and SA being rich in –OH groups. PVA also assisted the blend formation by retaining the crystallinity in blends comparable with pure GG and SA. The blended hydrogels showed slight shifting in peaks that were found in the pristine polymers. GA-03 displayed sharp peaks at 8.15° and 29.5° while GA-04 and GA-05 exhibited 8.06°, 29.6° and 8.01° respectively which confirmed the crystallinity of the hydrogels.

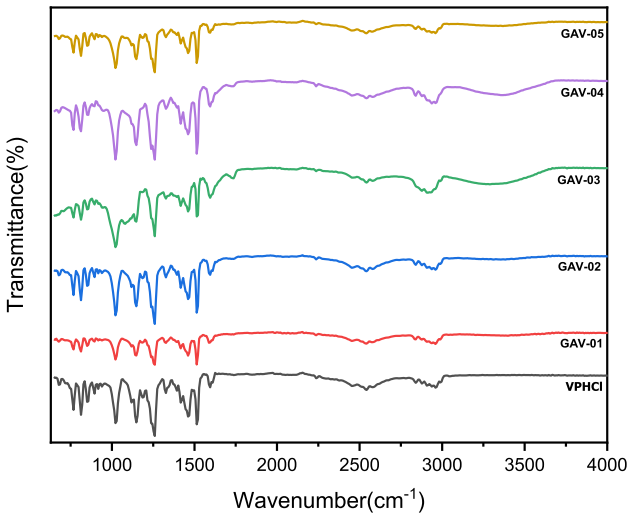

Fig. 3 FTIR spectra of VP-HCl and drug loaded blends.

3.3. Surface analysis

The surface roughness of blended hydrogels was determined by AFM analysis (Table 2), where root mean square (S_q) and arithmetic mean height (S_a) values were taken in account as roughness parameters. The S_q values were estimated to be 15.2, 31.8 and 61.8 nm for GA-03, GA-04 and GA-05 respectively. These higher values are indicative of change in surface topology of blended hydrogels. The cluster in blended hydrogel GA-05 was associated with high S_q and S_a evident from the higher surface deformation as compared to the other hydrogels (Fig. 5c). Lower S_q values observed in GA-03 and GA-04 indicated the smooth surface (Figs. 5a and 5b). It is

Table 1 FTIR data of blended hydrogels (GA-01 to GA-05).

Sample code	OH str cm^{-1}	C–H str cm^{-1}	C–O–C str cm^{-1}	1–4 linkage (mann/mann)	COO^- Asymm. str cm^{-1}	COO^- Symm. str cm^{-1}
GG	3272	2892	1148	760	–	–
SA	3257	2829	1088	–	1565	1423
PVA	3295	2914	1028	–	–	–
GA-01	3265	2892	1021	872	1595	1408
GA-02	3257	2922	1021	879	1595	1416
GA-03	3265	2922	1021	872	1595	1416
GA-04	3309	2937	1021	872	1595	1416
GA-05	3250	2922	1013	879	–	–

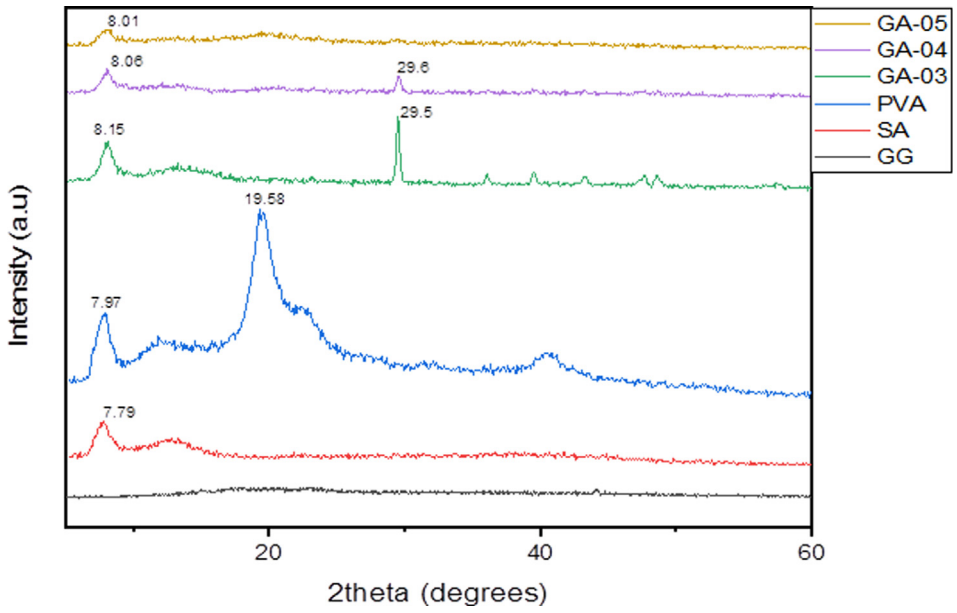

Fig. 4 XRD Spectra of pristine polymers and blended hydrogels.

Table 2 AFM data of blended hydrogels (GA-01 to GA-05) indicative of surface roughness.

Sample Codes	Blends Composition GG-SA-PVA(g)	Root Mean square (S_q) (nm)	Max. peak height (S_p) (nm)	Max. Valley depth (S_v) (nm)	Maximum height (S_z) (nm)	Arithmetic mean height (S_a) (nm)
GA-01	0.0:0.8:0.2					
GA-02	0.2:0.6:0.2	15.2	58.3	39.5	97.8	12.1
GA-03	0.4:0.4:0.2	31.8	82.5	88	171	26.0
GA-04	0.6:0.2:0.2					
GA-05	0.8:0.0:0.2	61.8	167	144	311	50.5

concluded that the blending of polymers induced roughness in the blended hydrogels. These results are in complete agreement with swelling behavior all hydrogels which demonstrated water retaining ability of blended hydrogels. The maximum swelling capacity of GA-05 has highest agglomeration that is evident of effective polymeric interactions. In GA-01, blends showed hydrophilic behavior and completely dissolved in water. SEM analysis is useful to study surface morphology, size, crystallinity and the positions of phases in the prepared hydrogels. SEM images of all the blended hydrogels showed the overall porous structure (Fig. 6). The SEM results were in accordance with the drug delivery results where porosity of the blends increases the swelling and entrapment of the drug inside the pores.

3.4. Thermal analysis

Thermogravimetry analysis (TGA) demonstrates the effect of temperature on the stability of blended hydrogels. TGA deals with the gradual change in mass of sample with increasing temperature (He et al., 2020; Hu et al., 2018; Hu et al., 2020c). Typical weight losses of the samples along with initial and final degradation temperatures were recorded. Thermo gravimetric analyses of blended hydrogels have been conducted at 25–550 °C. In TGA curves (Fig. 7) of blended hydrogels, the first light peak was due to dehydration followed by a second large plateau observed at 235, 249 and 283 °C was attributed to the degradation of the blended hydrogels of GA-03, GA-04 and GA-05 respectively.

The guar gum thermogram curve showed the gradual loss of weight directly proportional to the increase of temperature in the range of 50–110 °C associated to the gradual loss of water. The polymer becomes stable after this temperature range and up to 259.2 °C without any mass change (Table 3). TGA curve of SA showed initially a dehydration step followed by two overlapping peaks at 198 and 587 °C which correspond to the decomposition and sodium carbonate formation. TGA curve of PVA shows a significant endothermic peak at 205 °C. It is evident from the results that blending did not affect the stability of the pristine polymers in the course of hydrogel formation (Bosio et al., 2014). DSC thermograms of the blended hydrogels showed the strong exothermic peaks

at 541–543 °C showing crystallinity in the blended hydrogels (Fig. 8). These findings were in accordance with the XRD results of the blended hydrogels.

3.5. Swelling properties

Swelling is an important feature that reflects the water holding capacity and drug release behavior of the polymeric materials. Therefore, in this study, the swelling behavior of blended hydrogels was determined in deionized water and buffer solutions of pH 1.2 and 7.4. It was observed that the sample GA-04 and GA-05 showed the maximum swelling in water (Table 4). Sample GA-04 showed the best swelling which refers to the excellent networking of GG, SA and PVA while in GA-05 guar gum formed firm polymeric network with PVA. Thus, blends have increased hydrophobic character that helps them to retain water. It was observed that the swelling degree of hydrogels was higher in pH 7.4 than that in pH 1.2. The increased swel-

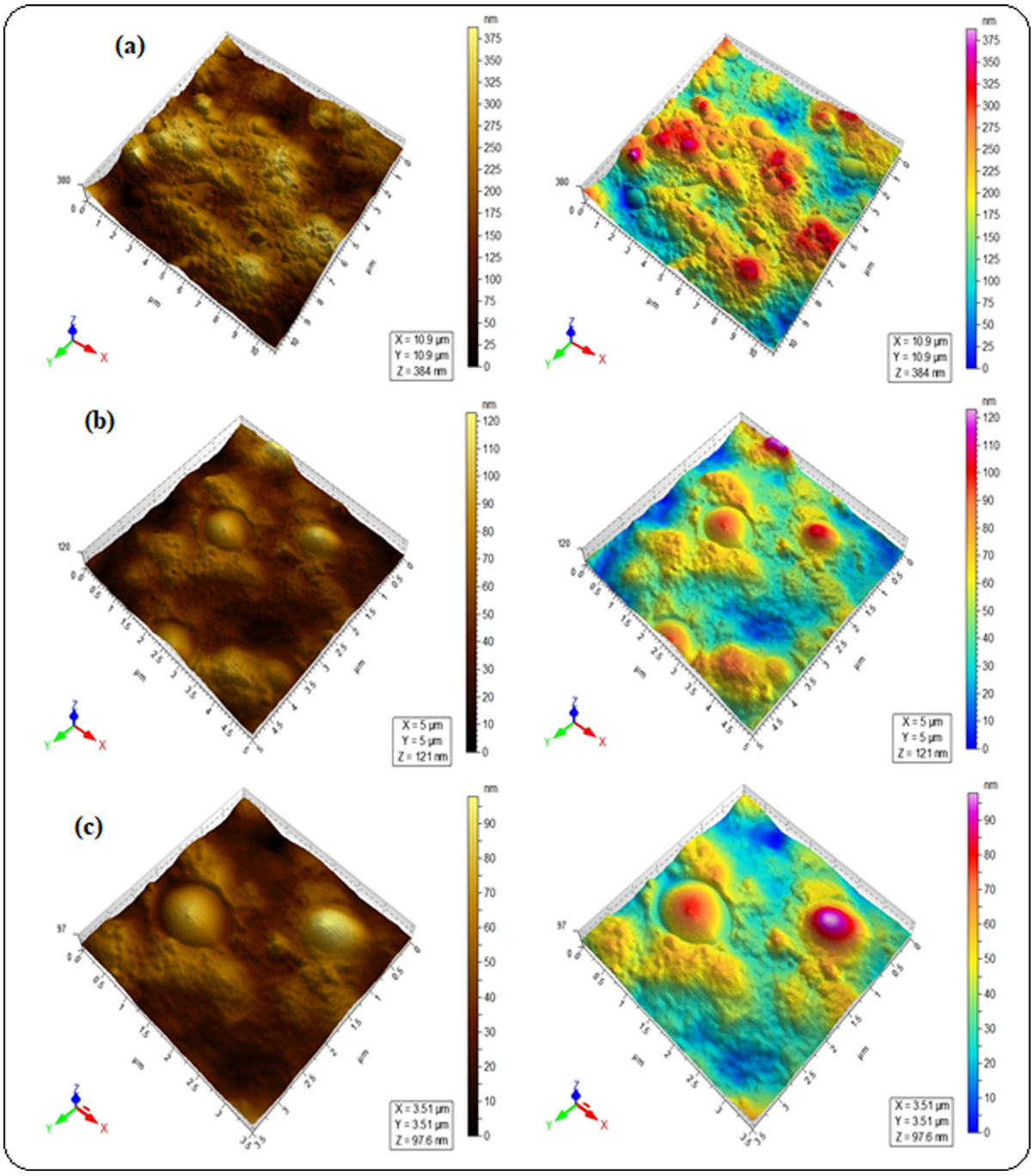

Fig. 5a AFM micrographs of blended hydrogels for the sample GA-03 (a) 2.5 µm, (b) 1 µm and (c) 0.75 µm.

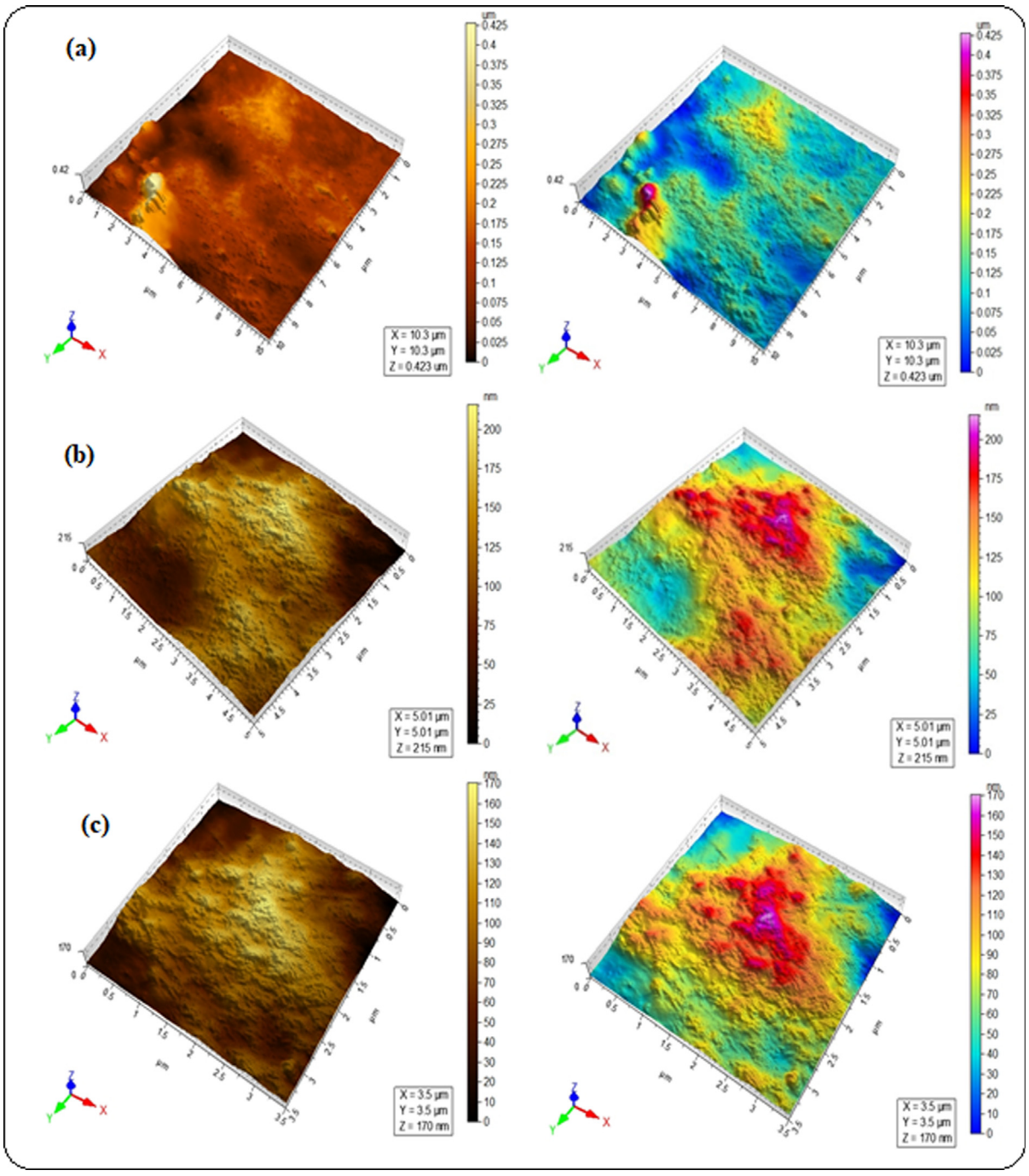

Fig. 5b AFM micrographs of blended hydrogels for the sample GA-04 (a) 2.5 µm, (b) 1 µm and (c) 0.75 µm.

ling of blended hydrogels in pH 7.4 may be attributed to the presence of bulk hydroxyl groups involved in H-bonding with carboxylate anion of SA in the hydrogel networks. In the acidic medium (pH 1.2), carboxylate anions are converted to –COOH groups and resulted in longer intermolecular distances which lower swelling degree of blended hydrogels. The characteristic variation of swelling ratio with pH of external medium illustrates the good pH responsive behavior of the blended hydrogels. These results revealed that blended hydrogels could be used as effective drug delivery carriers that show pH-dependent drug release behavior (Sullad et al., 2010).

3.6. Drug load and release efficiency

DL and DLE of the blended hydrogels range from 54 to 61.5% and 72–82% respectively (Table 5), revealed the gradual increase in the drug loading efficiency from GAV-02 to GAV-05. It is due to the increased number of hydrophilic groups which enhanced the intramolecular H-bonding in the

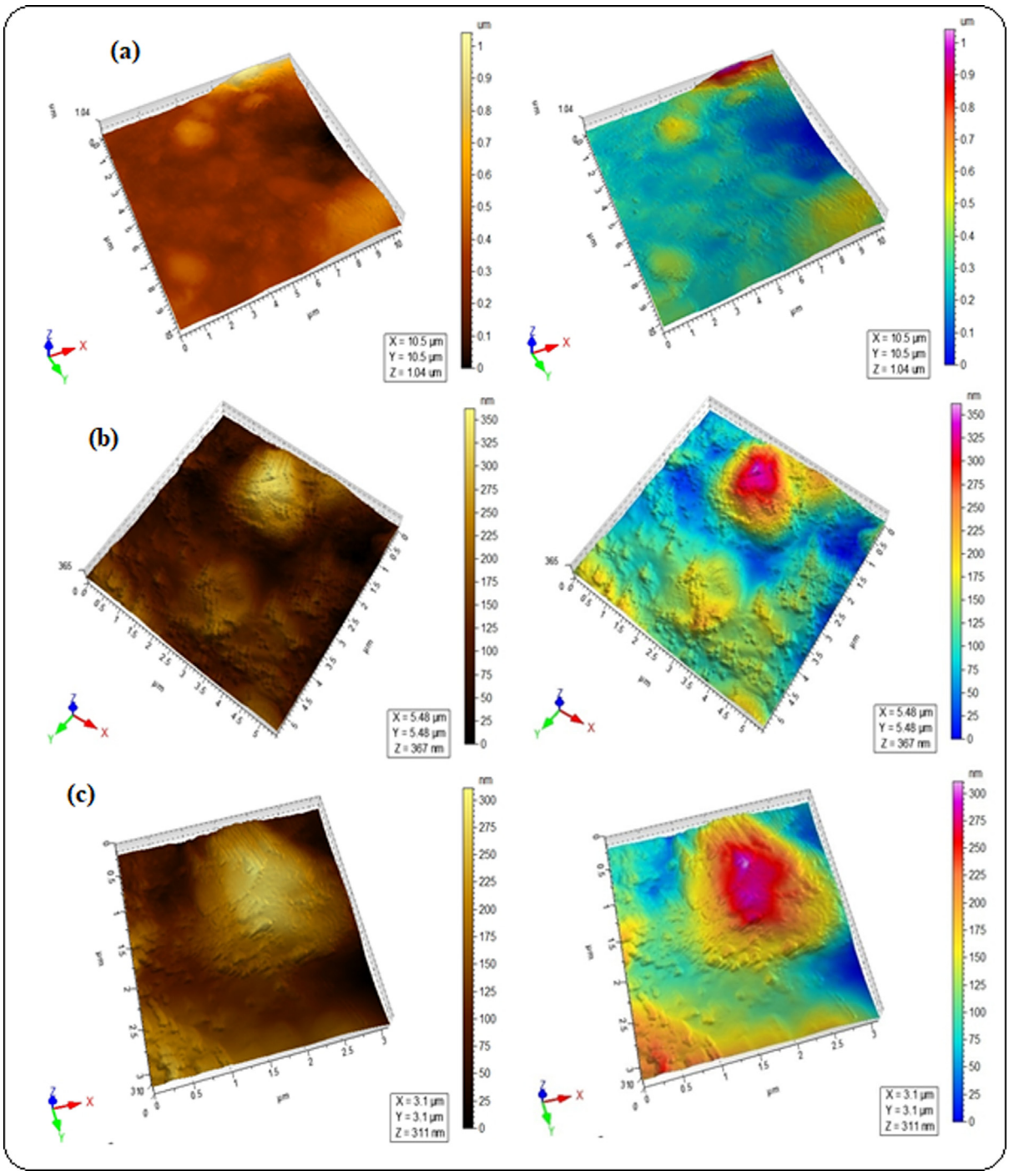

Fig. 5c AFM micrographs of blended hydrogels for the sample GA-05 (a) 2.5 µm, (b) 1 µm and (c) 0.75 µm.

blends which help to entrap the drug. GA-01 was not loaded with drug because it was completely dissolved in the swelling medium. The drug release studies have been conducted on the basis of normal pH environment of the gastrointestinal tract (GIT) that changes from pH 1.2 (acidic in the stomach) to 7.4 (alkaline in the intestine). Thus, this prime factor is substantially responsible for controlled release of the drug establishing these blends as pH-sensitive hydrogels. At lower pH, less than 17% VP-HCl released from the blended hydrogels which is much lesser as compared to release at pH 7.4 (94%) up to 12 h (Fig. 9). The change in the release of VP-HCl at two different pH levels is due to the variation in the swelling behavior of the blended hydrogels. The drug being water-soluble released from the blended hydrogels as the water diffuses into the polymeric network. This causes the swelling of the hydrogel and dissolution of the drug in the solution. Consequently, at lower pH it becomes very difficult for the VP-HCl to diffuse out of the hydrogels since the swelling ratio is very

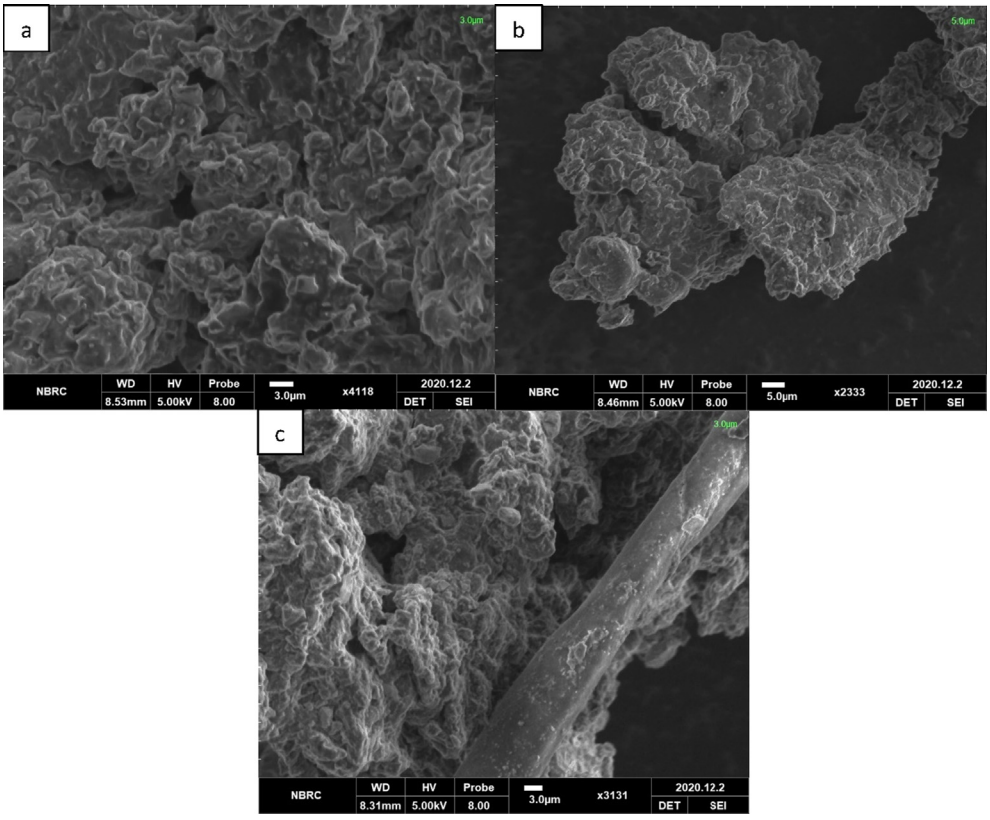

Fig. 6 SEM Images of the blended hydrogels GA-03 (a), GA-04 (b) and GA-05 (c).

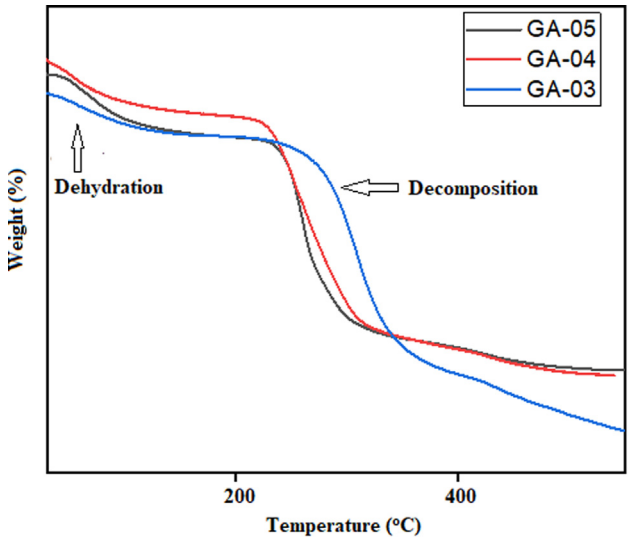

Fig. 7 TGA Thermograms of blended hydrogels showing the effect of temperature on stability.

Table 3 Onset and End set decomposition temperatures of blended hydrogels.

Sample Code	Onset decomposition temperature (°C)	End set decomposition temperature (°C)	Weight loss (%)
GA-03	235	290	65.7
GA-04	249	313	67
GA-05	283	344	77

small. VP-HCl migrated from the hydrogel network at pH 7.4 due to increased swelling phenomenon, hence prominent release of the drug was observed. According to previous studies, VP-HCl drug release potential was carried out exploiting the grafted copolymer pAAm-g-GG for 3–4 h (Soppirnath and Aminabhavi, 2002). Similar study was performed on super porous hydrogels of acrylamide and sodium alginate, which displayed fast drug release (up to 60%) in 30 min and further sustained until 24 h (Nagpal et al., 2013b). In the present study, the controlled release of VP-HCl was far better than that reported in literature. Hence, these hydrogels are proved to be efficient for drug release in control manner and have potential biomedical applications.

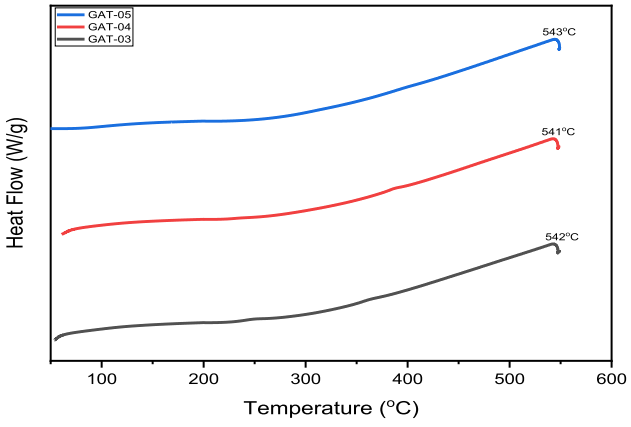

Fig. 8 DSC Thermograms of Blended Hydrogels.

Table 4 Swelling behavior of blended hydrogels (GA-02 to GA-05).

Samples	pH Scale	Time (min)						
		15	30	45	60	75	90	105
GA-02	1.2	835 ± 0.5	835 ± 0.1	837 ± 0.2	838 ± 0.2	840 ± 0.6	842 ± 0.2	842 ± 0.3
	7.0	957 ± 0.2	960 ± 0.4	960 ± 0.3	961 ± 0.3	961 ± 0.7	962 ± 0.2	963 ± 0.2
	7.4	1002 ± 0.3	1003 ± 0.4	1003 ± 0.1	1004 ± 0.2	1004 ± 0.1	1007 ± 0.5	1007 ± 0.1
GA-03	1.2	929 ± 0.5	930 ± 0.2	938 ± 0.1	939 ± 0.2	946 ± 0.1	946 ± 0.4	948 ± 0.4
	7.0	1152 ± 0.3	1159 ± 0.3	1168 ± 0.6	1168 ± 0.5	1168 ± 0.3	1172 ± 0.5	1172 ± 0.2
	7.4	1220 ± 0.2	1220 ± 0.3	1221 ± 0.5	1223 ± 0.5	1222 ± 0.2	1224 ± 0.2	1226 ± 0.2
GA-04	1.2	1708 ± 0.2	1709 ± 0.4	1710 ± 0.5	1716 ± 0.3	1718 ± 0.3	1718 ± 0.3	1719 ± 0.3
	7.0	1929 ± 0.1	1932 ± 0.4	1936 ± 0.4	1936 ± 0.4	1937 ± 0.0	1941 ± 0.3	1941 ± 0.2
	7.4	2006 ± 0.5	2006 ± 0.3	2007 ± 0.0	2007 ± 0.1	2009 ± 0.2	2009 ± 0.2	2010 ± 0.2
GA-05	1.2	1718 ± 0.4	1720 ± 0.3	1720 ± 0.3	1726 ± 0.3	1726 ± 0.1	1728 ± 0.1	1729 ± 0.4
	7.0	1940 ± 0.4	1941 ± 0.5	1941 ± 0.5	1944 ± 0.5	1944 ± 0.5	1945 ± 0.5	1945 ± 0.4
	7.4	2029 ± 0.2	2035 ± 0.2	2035 ± 0.4	2038 ± 0.1	2040 ± 0.3	2041 ± 0.3	2040 ± 0.3

Table 5 DL and DLE of the drug loaded blended hydrogels.

Sample code	DL%	DLE%
GAV-02	54 ± 0.2	72 ± 0.4
GAV-03	57 ± 0.2	76 ± 0.5
GAV-04	60 ± 0.5	80 ± 0.5
GAV-05	61.2 ± 0.3	82 ± 0.3

3.7. Mechanism of drug release

The model which best fits the data of drug release was investigated by the values of correlation coefficient (r). The values of r nearer to 1 are standard for selection of most suitable model.

It was evident from Table 6 that values of r for zero-order were found to be higher than those of the first order kinetics which revealed that blended hydrogels followed the first order kinetics. Higuchi model indicated the higher degree of correlation coefficient (r) which showed that the mechanism of drug release from the blended hydrogels was diffusion controlled. Furthermore, Krosmeyer-Peppas model described the type of diffusion mechanism for the release of drug. The values of release exponent 'n' (Table 7) indicated that the mechanism of drug release was non-Fickian diffusion controlled (Ranjha et al., 2010).

4. Conclusion

Guar gum based biodegradable hydrogels have been successfully prepared and employed as pH responsive drug delivery system. All the blends are thermally stable and showed the controlled release of the antihypertensive drug (94%) upto 12 h at pH 7.4 and follow non-Fickian diffusion controlled mechanism. The release of verapamil hydrochloride is much better in magnitude as compared to already reported hydrogels. It has been concluded that prepared hydrogels can be employed for biomedical applications.

CRediT authorship contribution statement

Hina Daud: Methodology, Investigation, Software, Writing - Original draft preparation. **Ambreen Ghani:**

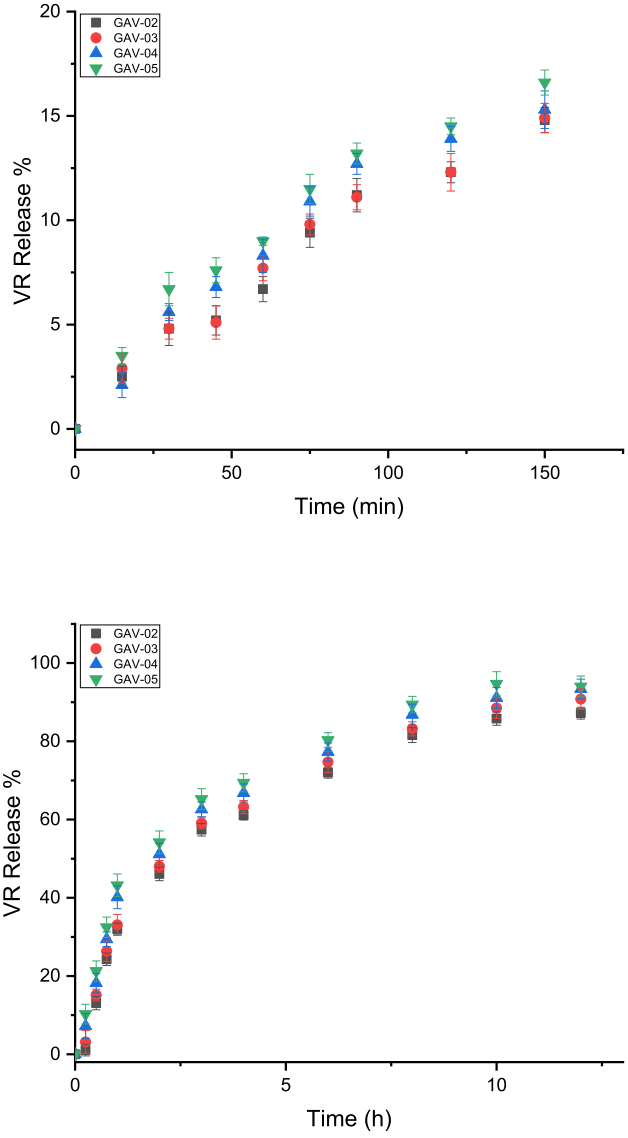

Fig. 9 Drug release profile (%) of blended hydrogels at pH (a) 1.2, (b) 7.4.

Table 6 Drug release kinetic data of blended hydrogels for zero-order, 1st order and Higuchi model kinetics.

Sample Code	pH	Zero order kinetics		First order kinetics		Higuchi equation	
		$K_o(h^{-1})$	r	$K_1(h^{-1})$	r	K_h (h^{-1})	r
GAV-02	1.2	0.283	0.9939	2.049	0.9427	0.07	0.9941
	7.4	0.595	0.9915	1.074	0.8567	0.59	0.9914
GAV-03	1.2	0.263	0.9937	1.969	0.9330	0.07	0.9938
	7.4	0.656	0.9932	0.699	0.8697	0.59	0.9931
GAV-04	1.2	0.240	0.9928	2.002	0.9178	0.07	0.9927
	7.4	0.770	0.9928	0.339	0.8479	0.59	0.9928
GAV-05	1.2	0.327	0.9899	1.699	0.8919	0.08	0.9897
	7.4	0.868	0.9902	0.173	0.8248	0.70	0.9902

Table 7 Drug release kinetic data of blended hydrogels for Krosmeyer-Peppas equation.

Sample code	pH	K_{kp} (h^{-1})	Release exponent (n)	r	Order of Release
GAV-02	1.2	0.075	0.7088	0.9816	Non-Fickian
	7.4	0.178	0.9729	0.8369	Non-Fickian
GAV-03	1.2	0.082	0.7234	0.9873	Non-Fickian
	7.4	0.196	0.718	0.9201	Non-Fickian
GAV-04	1.2	0.075	0.8409	0.9758	Non-Fickian
	7.4	0.196	0.9644	0.7921	Non-Fickian
GAV-05	1.2	0.097	0.6943	0.9423	Non-Fickian
	7.4	0.337	0.5317	0.9403	Non-Fickian

Supervision, Conceptualization. **Dure Najaf Iqbal:** Data curation, Analysis. **Nasir Ahmad:** Data curation, Analysis. **Saliha Nazir:** Methodology, Investigation, Software, Writing - Original draft preparation. **Mahnoor Jan Muhammad:** Visualization. **Erum Akbar Hussain:** Supervision, Conceptualization. **Arif Nazir:** Software, Validation, Writing - review & editing. **Munawar Iqbal:** Software, Validation, Writing - review & editing.

Declaration of Competing Interest

The authors declare that they have no known competing financial interests or personal relationships that could have appeared to influence the work reported in this paper.

Acknowledgements

Authors acknowledge the facilities provided by Central Research Laboratories, Lahore College for Women University, Lahore, Pakistan.

References

Abbas, M., Hussain, T., Arshad, M., Ansari, A.R., Irshad, A., Nisar, J., Hussain, F., Masood, N., Nazir, A., Iqbal, M., 2019. Wound healing potential of curcumin cross-linked chitosan/polyvinyl alcohol. Int. J. Biol. Macromol. 140, 871–876.

Abdullah, N.H., Wan Abu Bakar, W.A., Hussain, R., Bakar, M.B., van Esch, J.H., 2018. Effect of homogeneous acidic catalyst on mechanical strength of trishydrazone hydrogels: Characterization and optimization studies. Arab. J. Chem. 11, 635–644.

Ahmad, A., Mubharak, N.M., Naseem, K., Tabassum, H., Rizwan, M., Najda, A., Kashif, M., Bin-Jumah, M., Hussain, A., Shaheen, A., Abdel-Daim, M.M., Ali, S., Hussain, S., 2020. Recent advancement and development of chitin and chitosan-based nanocomposite for drug delivery: Critical approach to clinical research. Arab. J. Chem. 13, 8935–8964.

Ailincai, D., Gavril, G., Marin, L., 2020. Polyvinyl alcohol boric acid–A promising tool for the development of sustained release drug delivery systems. Mater. Sci. Eng. C 107, 110316.

Akbari, K., Moghadam, P.N., Behrouzi, M., Fareghi, A.R., 2020. Synthesis of three-dimensional hydrogels based on poly(glycidyl methacrylate-alt-maleic anhydride): Characterization and study of furosemide drug release. Arab. J. Chem. 13, 8723–8733.

Alpaslan, D., Dudu, T.E., Aktaş, N., 2021. Synthesis and characterization of novel organo-hydrogel based agar, glycerol and peppermint oil as a natural drug carrier/release material. Mater. Sci. Eng. C 118, 111534.

Amer, M.W., Awwad, A.M., 2021. Green synthesis of copper nanoparticles by *Citrus limon* fruits extract, characterization and antibacterial activity. Chem. Int. 7, 1–8.

Aminabhavi, T.M., Nadagouda, M.N., Joshi, S.D., More, U.A., 2014. Guar gum as platform for the oral controlled release of therapeutics. Expert Opin. Drug Deliv. 11, 753–766.

Ata, S., Rasool, A., Islam, A., Bibi, I., Rizwan, M., Azeem, M.K., Qureshi, A.u.R., Iqbal, M., 2020. Loading of Cefixime to pH sensitive chitosan based hydrogel and investigation of controlled release kinetics. Int. J. Biol. Macromol. 155, 1236–1244.

Awwad, A.M., Amer, M.W., 2020. Biosynthesis of copper oxide nanoparticles using Ailanthus altissima leaf extract and antibacterial activity. Chem. Int. 6, 210–217.

Bosio, V.E., Basu, S., Abdullha, F., Villalba, M.E.C., Güida, J.A., Mukherjee, A., Castro, G.R., 2014. Encapsulation of Congo Red in carboxymethyl guar gum–alginate gel microspheres. React. Funct. Polym. 82, 103–110.

Boukhouya, I., Bakouri, H., Abdelmalek, I., Amrane, M., Guemra, K., 2018. Controlled release of amoxicillin from PMMA and poly (butylsuccinate) microspheres. Chem. Int. 4, 120–129.

Campos, J.C., Cunha, D., Ferreira, D.C., Reis, S., Costa, P.J., 2021. Oromucosal precursors of in loco hydrogels for wound-dressing and drug delivery in oral mucositis: Retain, resist, and release. Mater. Sci. Eng. C 118, 111413.

Dhand, A.P., Galarraga, J.H., Burdick, J.A., 2020. Enhancing Biopolymer Hydrogel Functionality through Interpenetrating Networks. Trend. Biotechnol. (aheaf of print). https://doi.org/10.1016/j.tibtech.2020.08.007.

George, M., Abraham, T., 2007. pH sensitive alginate–guar gum hydrogel for the controlled delivery of protein drugs. Int. J. Pharma. 335, 123–129.

Grekhnyova, E.V., Kudryavtseva, T.N., Kometiani, I.B., Velyaev, Y. O., 2017. Microencapsulation of furacilin as a method of creating new medicinal forms, possessing with increased biological accessibility and prolongable effect. Asian J. Pharma. 11, S920.

He, J., Ni, F., Cui, A., Chen, X., Deng, S., Shen, F., Huang, C., Yang, G., Song, C., Zhang, J., Tian, D., Long, L., Zhu, Y., Luo, L., 2020. New insight into adsorption and co-adsorption of arsenic and tetracycline using a Y-immobilized graphene oxide-alginate hydrogel: Adsorption behaviours and mechanisms. Sci. Total Environ. 701, 134363.

Hu, X., Wang, Y., Zhang, L., Xu, M., 2020a. Construction of self-assembled polyelectrolyte complex hydrogel based on oppositely charged polysaccharides for sustained delivery of green tea polyphenols. Food Chem. 306, 125632.

Hu, X., Wang, Y., Zhang, L., Xu, M., 2020b. Formation of self-assembled polyelectrolyte complex hydrogel derived from salecan and chitosan for sustained release of Vitamin C. Carbohyd. Polym. 234, 115920.

Hu, X., Wang, Y., Zhang, L., Xu, M., Dong, W., Zhang, J., 2017. Redox/pH dual stimuli-responsive degradable Salecan-g-SS-poly (IA-co-HEMA) hydrogel for release of doxorubicin. Carbohyd. Polym. 155, 242–251.

Hu, X., Wang, Y., Zhang, L., Xu, M., Zhang, J., Dong, W., 2018. Photopatterned salecan composite hydrogel reinforced with α-Mo2C nanoparticles for cell adhesion. Carbohyd. Polym. 199, 119–128.

Hu, X., Yan, L., Wang, Y., Xu, M., 2020c. Smart and functional polyelectrolyte complex hydrogel composed of salecan and chitosan lactate as superadsorbent for decontamination of nickel ions. Int. J. Biol. Macromol. 165, 1852–1861.

Iqbal, D.N., Nazir, A., Iqbal, M., Yameen, M., 2020a. Green synthesis and characterization of carboxymethyl guar gum: Application in textile printing technology. Green Proces. Synth. 9, 212–218.

Iqbal, D.N., Shafiq, S., Khan, S.M., Ibrahim, S.M., Abubshait, S.A., Nazir, A., Abbas, M., Iqbal, M., 2020b. Novel chitosan/guar gum/PVA hydrogel: Preparation, characterization and antimicrobial activity evaluation. Int. J. Biol. Macromol. 164, 499–509.

Iqbal, D.N., Tariq, M., Khan, S.M., Gull, N., Sagar Iqbal, S., Aziz, A., Nazir, A., Iqbal, M., 2020c. Synthesis and characterization of chitosan and guar gum based ternary blends with polyvinyl alcohol. Int. J. Biol. Macromol. 143, 546–554.

Iqbal, M., Khera, R.A., 2015. Nanoscale bioactive glasses and their composites with biocompatible polymers. Chem. Int. 1, 17–34.

Kajjari, P.B., Manjeshwar, L.S., Aminabhavi, T.M., 2012. Novel pH- and temperature-responsive blend hydrogel microspheres of sodium alginate and PNIPAAm-g-GG for controlled release of isoniazid. Aaps Pharm. 13, 1147–1157.

Mauri, E., Salvati, A., Cataldo, A., Mozetic, P., Basoli, F., Abbruzzese, F., Trombetta, M., Bellucci, S., Rainer, A., 2021. Graphene-laden hydrogels: A strategy for thermally triggered drug delivery. Mater. Sci. Eng. C 118, 111353.

Nagpal, M., Singh, S.K., Mishra, D., 2013. Synthesis characterization and in vitro drug release from acrylamide and sodium alginate based superporous hydrogel devices. Int. J. Pharm. Investigat. 3, 131.

Nesrinne, S., Djamel, A., 2017. Synthesis, characterization and rheological behavior of pH sensitive poly(acrylamide-co-acrylic acid) hydrogels. Arab. J. Chem. 10, 539–547.

Paarakh, M.P., Jose, P.A., Setty, C., Christoper, G., 2018. Release kinetics–concepts and applications. Int. J. Pharm. Res. Tech. 8, 12–20.

Pallavi, K., Pallavi, T., 2017. Formulation and evaluation of fast dissolving films of eletriptan hydrobromide. Int. J. Curr. Pharma. Res. 9, 59.

Paradee, N., Thanokiang, J., Sirivat, A., 2021. Conductive poly(2-ethylaniline) dextran-based hydrogels for electrically controlled diclofenac release. Mater. Sci. Eng. C 118, 111346.

Parandhama, A., Madhavi, C., Maruthi, Y., Babu, P.K., Reddy, O.S., Rao, K.C., Subha, M., 2017. Controlled Release of Verapamil Hydrochloride, an Antihypertensive Drug from the Interpenetrating Blend Microparticles of Gelatin and Gellan Gum. Indian J. Adv. Chem. Sci. 5, 176–184.

Park, S.-B., Lih, E., Park, K.-S., Joung, Y.K., Han, D.K., 2017. Biopolymer-based functional composites for medical applications. Prog. Polym. Sci. 68, 77–105.

Prasanth, A.G., Kumar, A.S., Shruthi, B.S., Subramanian, S., 2020. Kinetic study and in vitro drug release studies of nitrendipine loaded arylamide grafted chitosan blend microspheres. Mater. Res. Expres. 6, 125427.

Rangaraj, G., Kishore, N., Dhanalekshmi, U.M., Raja, M.D., Reddy, P.N., 2010. Design and study of formulation variables affecting drug loading and its release from Alginate beads. J. Pharma. Sci. Res. 2, 77–81.

Ranjha, N.M., Ayub, G., Naseem, S., Ansari, M.T., 2010. Preparation and characterization of hybrid pH-sensitive hydrogels of chitosan-co-acrylic acid for controlled release of verapamil. J. Mater. Sci. Mater. Med. 21, 2805–2816.

Rasool, A., Ata, S., Islam, A., Rizwan, M., Azeem, M.K., Mehmood, A., Khan, R.U., Mahmood, H.A., 2020. Kinetics and controlled release of lidocaine from novel carrageenan and alginate-based blend hydrogels. Int. J. Biol. Macromol. 147, 67–78.

Samarth, N.B., Kamble, V., Mahanwar, P., Rane, A., Abitha, V., 2015. A historical perspective and the development of molecular imprinting polymer-A review. Chem. Int. 4, 202–210.

Seeli, D.S., Dhivya, S., Selvamurugan, N., Prabaharan, M., 2016. Guar gum succinate-sodium alginate beads as a pH-sensitive carrier for colon-specific drug delivery. Int. J. Biol. Macromol. 91, 45–50.

Sekhar, E.C., Rao, K.K., Raju, R.R., 2011. Chitosan/guargum-g-acrylamide semi IPN microspheres for controlled release studies of 5-Fluorouracil. J. Appl. Pharma. Sci. 1, 199.

Shammout, M.W., Awwad, A.M., 2021. A novel route for the synthesis of copper oxide nanoparticles using Bougainvillea plant flowers extract and antifungal activity evaluation. Chem. Int. 7, 71–78.

Sharma, G., Sharma, S., Kumar, A., Ala'a, H., Naushad, M., Ghfar, A.A., Mola, G.T., Stadler, F.J., 2018. Guar gum and its composites as potential materials for diverse applications: A review. Carbohyd. Polym. 199, 534–545.

Soppirnath, K.S., Aminabhavi, T.M., 2002. Water transport and drug release study from cross-linked polyacrylamide grafted guar gum hydrogel microspheres for the controlled release application. Eur. J. Pharma. Biopharma. 53, 87–98.

Suardi, M., Wangi, Q., Salman, Zaini, E., Akmal, D., 2016. Microencapsulation of Verapamil Hydrochloride using Poly (3-hidroxybutyrate) as Coating Materials by Solvent Evaporation Method. Res. J. Pharma. Biol. Chem. Sci. 7, 1725–1732.

Sullad, A.G., Manjeshwar, L.S., Aminabhavi, T.M., 2010. Novel pH-sensitive hydrogels prepared from the blends of poly (vinyl alcohol) with acrylic acid-graft-guar gum matrixes for isoniazid delivery. Ind. Eng. Chem. Res. 49, 7323–7329.

Thakur, S., Sharma, B., Verma, A., Chaudhary, J., Tamulevicius, S., Thakur, V.K., 2018. Recent progress in sodium alginate based sustainable hydrogels for environmental applications. J. Clean. Product. 198, 143–159.